MODELLING OF NONLINEAR DILATATION RESPONSE OF FLUIDS CONTAINING COLUMNS-Plastic and Shear Relaxation Considered

Bernd Wendlandt*
Department of Defence, Materials Research
Laboratory, DSTO, PO Box 50, Ascot Vale,
Victoria 3032, Australia

Abstract

The non-linear wave equation governing the propagation and scatter of dilatation waves in discontinuous media is presented and its Eulerian numerical analogue is used to study scatter of acoustic dilatation waves by columns and ducts in elastic and visco-elastic fluids. Plastic and visco-elastic relaxation mechanisms are considered. The spectral form of the wave equation is developed and used to discuss dispersion. Selected applications of the numerical analogue to simulation of scatter, propagation and echo attenuation are presented.

INTRODUCTION

A second order, partially implicit and alternating direction Eulerian numerical approximation to the parabolic, first order non-linear wave equation is used to compute scatter of dilatations from inhomogeneities in material moduli and density. Spectral analysis is used to discuss the dispersive effect material inhomogeneities have on travelling dilatational waves. The usefulness of the scheme is illustrated by simulating the propagation of a Gaussian shaped dilatational pulse around an elbow in a duct immersed and radially out of a cylinder in an elastic fluid and by computing the scatter of dilatations from air columns in elastic fluids. Finally, the reflection of dilatations from a row of double and single wedge shaped air columns in a fictitious plastic-visco-elastic medium backed by a layer of air is calculated. The scheme considers plastic relaxation and visco-elastic relaxation due to compression and shear.

MODEL

The propagation of acoustic waves is governed by the laws of conservation of momentum and mass, and equation of state which relates the stress in a medium to the associated strain through material properties. The Hookean-Kelvin model [1] provides the simplest relationship between strain and stress, which, when applied to compression and shear separately, yields a stress-strain

*5 Cumberland Ct, Annapolis, MD 21401, Telephone: (301) 267 6653.

relationship which reflects observed plastic relaxation and visco-elastic relaxation in dilatation and shear. This relationship can be written as

$$\sigma_{ij} + \beta_\sigma \frac{\partial \sigma_{ij}}{\partial t} = \lambda \left(1 + \beta_\lambda \frac{\partial}{\partial t}\right) \epsilon_{mm} \delta_{ij} + 2\mu \left(1 + \beta_\mu \frac{\partial}{\partial t}\right) \epsilon_{ij} \qquad (1)$$

where σ_{ij} is the stress tensor and ϵ_{ij} is the strain tensor. Material properties are described by λ,the first Lamé constant, and μ, the modulus of rigidity. The plastic and visco-elastic relaxation times of the material for direct and shear strains are β_σ, β_λ and β_μ respectively. The strain tensor is related to the displacement tensor u_i for small displacements by the linear expression $\epsilon_{ij} = (u_{i,j} + u_{j,i})/2$, where $u_{i,j}$ represents differentiation of tensor u_i with respect to displacement tensor x_j. This strain-displacement relationship provides an adequate description for material response to excitations when the strain is less than about 10%. Strain can vary rapidly with respect to distance at material interfaces [2], particularly when the acoustic or vibrational impedance varies significantly across the interface. The strain at the interface of materials with disparate acoustic impedances is more accurately modelled by the parabolic, or first order non-linear, approximation to the strain [3] and [4], which can be expressed as $\epsilon_{ij} = (u_{i,j} + u_{j,i} + u_{k,i}u_{k,j})/2$. Incorporation of this non-linear strain into Equation 1, enables the Hookean-Kelvin stress-strain constitutive equation to accurately model material responses for strain values up to 30%, [3]. In this approximation, σ_{ij} is known as the 2nd Piola-Kirchhoff stress tensor and ϵ_{ij} is known as the Green-Lagrangian strain tensor [3]. A linearized expression for the non-linear strain can be obtained from a first order extension of Taylor expansion definition of the strain-displacement definition [5] which yields

$$\epsilon_{ij} \approx \frac{1}{2}\{u_{i,j} + u_{j,i} + \frac{\partial(u_{i,j} + u_{j,i})}{\partial x_j} \delta x_j\} \qquad (2)$$

When this expression for the strain is substituted into Equation 1, a second order approximation in u to the non-linear constitutive law is obtained.

When $\lambda \gg \mu$ the propagation of an acoustic excitation in the medium may be described by the dilatation , Θ . Dilatation is defined by the divergence of the incremental displacement of the strain. In regions where the medium is uniform, the dilatation Θ is related to the pressure by $p = -\rho c^2 \Theta$, where ρ is the density and c is the speed of sound characterizing the medium. The propagation of the dilatation can be described by a wave equation derived from divergence of the law of conservation of momentum, $\rho \frac{\partial^2 u}{\partial t^2} = \frac{\partial \sigma_{ij}}{\partial x_j}$, and mass, $\frac{\partial \rho}{\partial t} = -\rho \frac{\partial \Theta}{\partial t}$, and combined with the above approximation to the non-linear constitutive law, Equation 1 and the non-linear strain Equation 2. This non-linear wave equation can be expressed, approximately, as

$$\rho \frac{\partial^2 \Theta}{\partial t^2} \approx \nabla^2\{(\lambda^* + <\mu^*>)(\Theta + \nabla\Theta \cdot \delta\vec{x})\} + \nabla \cdot (<\mu^*> \nabla\{\Theta + \nabla\Theta \cdot \delta\vec{x}\}) + Q_s \quad (3)$$

where $\lambda^* = \lambda(1 + \{\beta_\lambda - \beta_\sigma\}\frac{\partial}{\partial t})$ and $\mu^* = \mu(1 + \{\beta_\mu - \beta_\sigma\}\frac{\partial}{\partial t})$, and $\delta\vec{x}$ is an increment of expansion of the position vector of the spatial location (x, y, z). The density, ρ at position (x, y, z) and time t is related to the initial, unperturbed

density ρ_0 from the law of conservation of mass by $\rho \approx \rho_0(1 - \Theta + \Theta^2)$, to second order in Θ, which is assumed to be zero at time $t = 0$. The $< \mu^* >$ represents the average value of μ^* over a small volume of computational cell of the numerical analogue of Equation 3. This approximation is justified through the integral form of the divergence theorem [1].

The Q_s describes the scatter of dilatation waves by material inhomogeneities and can be written as

$$Q_s \approx -\frac{\nabla\rho}{\rho} \cdot [\nabla(\lambda^* + < \mu^* >)(\Theta + \nabla\Theta \cdot \delta\vec{x}) + < \mu^* > \nabla(\Theta + \nabla\Theta \cdot \delta\vec{x})] \quad (4)$$

The Q_s is a source term for the generation of dilatation wavelets at material discontinuities [1]. Shear losses dominate when $\mu\beta_\mu \frac{\partial}{\partial t} \gg \lambda\beta_\lambda \frac{\partial}{\partial t}$.

The non-linear wave equation, Equation 3, is dispersive and a spectral analysis [6] of Equation 3 shows that as dilatational waves interact with and are scattered by material inhomogeneities they may change their nature from travelling to damped and vice versa. If the dilatation wave, Θ is represented in complex formulation, where $\imath = \sqrt{-1}$, by

$$\Theta = \Theta_0 \exp \imath(\vec{k} \cdot \vec{x} - \omega t) \quad (5)$$

where $\vec{k}$ is the momentum vector, Θ_0 is the amplitude and ω the angular frequency of the wave, the spectrum form of Equation 3 may be written as the quadratic expression $ak^2 - \imath bk - c \approx 0$. The spectrum relation [6] for the momentum vector k is then in terms of material properties and angular frequency given by

$$k(\omega) \approx \pm\frac{\sqrt{4ac + b^2}}{2a} + \imath\frac{b}{2a} \quad (6)$$

where the coefficients

$$a = \lambda_\omega + 2 < \mu >_\omega + (2\nabla[\lambda_\omega + < \mu >_\omega] + \nabla < \mu >_\omega - \frac{\nabla\rho}{\rho}[\lambda_\omega + 2 < \mu >_\omega])\hat{k} \cdot \delta\vec{x} \quad (7)$$

and

$$b \approx \left[2\nabla(\lambda_\omega + < \mu >_\omega) + \nabla < \mu >_\omega - (\lambda_\omega + 2 < \mu >_\omega)\frac{\nabla\rho}{\rho}\right] \cdot \hat{k} + \left[\nabla^2(\lambda_\omega + < \mu >_\omega) - \frac{\nabla\rho}{\rho} \cdot \nabla(\lambda_\omega + < \mu >_\omega)\right] \hat{k} \cdot \delta\vec{x} \quad (8)$$

and

$$c = \rho\omega^2 + \nabla^2(\lambda_\omega + < \mu >_\omega) - \frac{\nabla\rho}{\rho} \cdot \nabla(\lambda_\omega + < \mu >_\omega) \quad (9)$$

Here the Lamé operators convert in frequency space to the complex parameters $\lambda_\omega = \lambda(1 + \imath\omega[\beta_\sigma - \beta_\lambda])$ and $\mu_\omega = \mu(1 + \imath\omega[\beta_\sigma - \beta_\mu])$. The terms $\hat{k}$ denote unit vectors of $\vec{k}$

Inspection of the exponential representation of Θ for a wave, Equation 5, shows that Θ is a travelling wave when $\vec{k}$ is real and is damped, or decays as $\exp -\vec{\kappa} \cdot \vec{x}$, when $\vec{k}$ is complex and $\vec{\kappa}$ represents the imaginary component of $\vec{k}$.

Equation 6 has at least one complex root for $\vec{k}$, even when plasticity and viscous effects are ignored, if the material properties are inhomogeneous and $b \neq 0$. Thus travelling waves may be damped, or decay exponentially, in elastic inhomogeneous materials. Waves whose frequencies, and direction of propagation relative to material interfaces, make $b^2 > 4ac$ are completely damped and do not propagate.

NUMERICAL ANALOGUE OF WAVE EQUATION

Equation 3 assumes that the material parameters are differentiable with respect to spatial coordinates. Their use in discontinuous media may require special consideration of boundary conditions to avoid any smearing of material interfaces. However, very acceptable solution schemes for wave equations have been obtained, [7] and [2], which do not require special treatment of boundary conditions and linear approximations in Θ are able to trace the propagation of acoustic Gaussian pulses and wave- packets through water-elastomer-air-elastomer-steel-water sandwiches to an accuracy of 95 to 98 %, Figure 1 and 2 which show superimposed snapshots of Gaussian pulses reflected and transmitted across interfaces. As the problems computed are one dimensional the more familiar particle displacement rather than dilatation is shown. However,

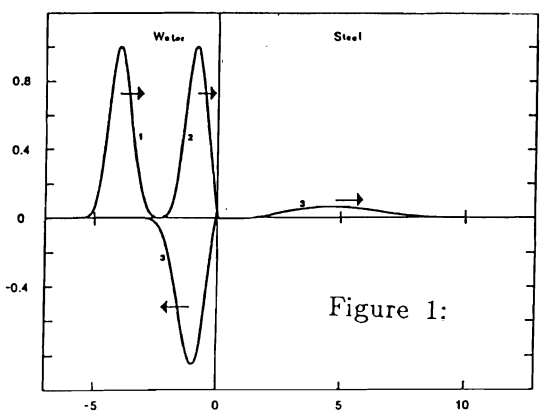

Figure 1:

Figure 1: Snapshot of Gaussian pulse reflected and transmitted at water/steel interface

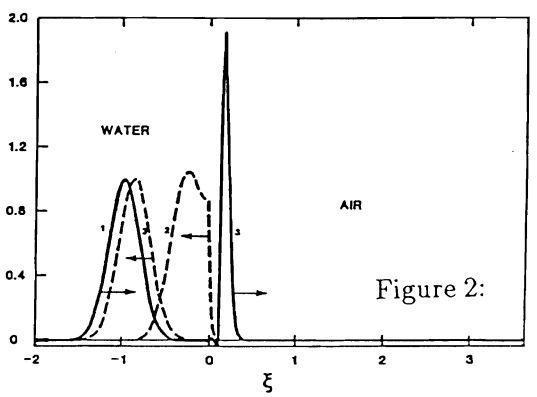

Figure 2:

Figure 2: Snapshot of Gaussian pulse reflected and transmitted at air/water interface

close inspection of the displacement variations at the material interfaces indicates that the waves are not very well approximated at the interface, although accurately away from the interface. This ability of the linear wave equation to model reflection and refraction from material interfaces accurately, without yielding accurate values of the functional at the interface is well known [7]. The distortions shown in Figures 1 and 2 indicate that strain variations across interfaces may be greater than 10% and that a non-linear form of the wave equation, which permits dilation to be approximated by a parabolic expression, is appropriate for accurate approximation to dilatations at the material interfaces. Accurate modelling of dilatations at interfaces is important in understanding composite material delamination under vibrational loading [8].

Using second order, centered differences for the derivatives of Equation 3

a numerical analogue was written in an explicit-implicit formulation [9], which can readily be integrated using the unconditionally stable alternating direction technique, ADI [10]. The ADI time steps the analogue equation to Equation 3 implicitly, first along one space dimension , leaving all terms involving differentiation along the other space dimension and the non-linear terms at the previous time level temporarily to provide an interim approximation to Θ. This process is repeated along the other space dimension, and Θ in the non- linear terms assume the value of the interim approximation to Θ. An updated value for Θ is considered to have been obtained after the completion of this second step [10].

CASE STUDIES

To illustrate the usefulness of Equation 3, and the resulting finite difference scheme, three case studies were carried out. First the scheme was used to simulate the propagation of a Gaussian shaped dilatation pulse, see Figure 3, around a curved duct immersed in water and of acoustic impedance equal to

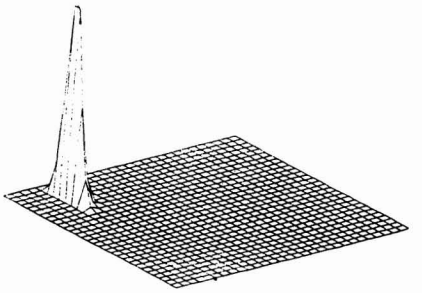

Figure 3: Initial Gaussian profile of pulse launched down duct.

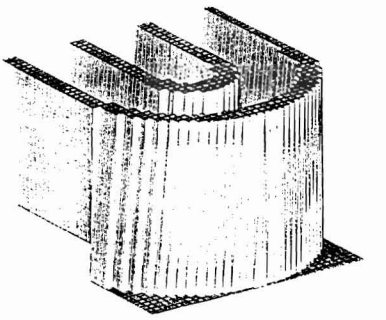

Figure 4: Density cross-section of duct elbow/water background

that of water. For ease of simulation, the density of the duct, see Figure 4

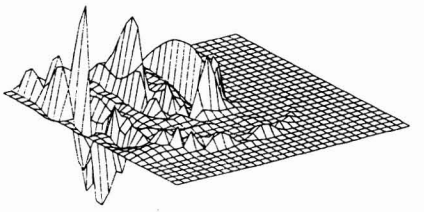

Figure 5: Snapshot of Gaussian pulse scattered in duct

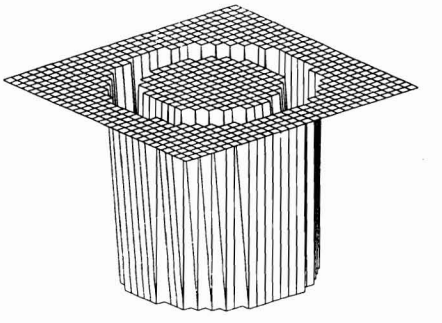

Figure 6: Speed of sound cross-section of cylinder/water background

, was taken to be four times that of water. The pulse was attenuated upon

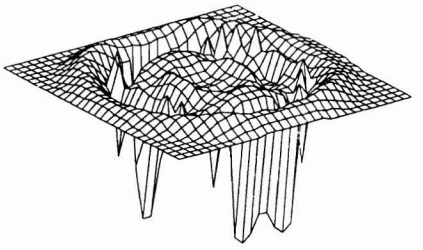

Figure 7: Snapshot of Gaussian pulse expanding through cylinder walls

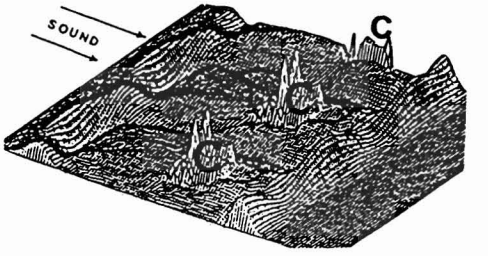

Figure 8: Snapshot of reflection and transmission of Gaussian shaped acoustic pulse by row of air filled square columns in water,pulse incident from upper left

scatter from the duct walls and very little is transmitted around the bend of the duct, see Figure 5. In the example displayed more dilatation is transmitted through the duct wall than around the duct bend at the time of the computation snapshot shown. This attenuation of the pulse is expected from the spectrum relation Equation 6. Second, the scheme was used to calculate the acoustic response of a cylinder immersed in water, and of material properties of the duct, see Figure 6, to a Gaussian pulse generated at time $t = 0$ along the axis of the cylinder. A snapshot of the radial expansion of the pulse and its penetration through and reflection from the cylinder wall is shown in Figure 7. As can be seen from Figure 7, the pulse radiates outward uniformly as expected and is partially reflected from the cylinder walls. The reflections are seen to be uneven, and rotate around the inside of the cylinder wall indicating that the reflections are not the first mode, or specular, reflections but are higher, circumferential modes. Thirdly, the scheme was used to calculate the acoustic

Figure 9: Snapshot of reflection and transmission of Gaussian shaped acoustic pulse by row of air filled cylindrical columns in water,pulse incident from upper left

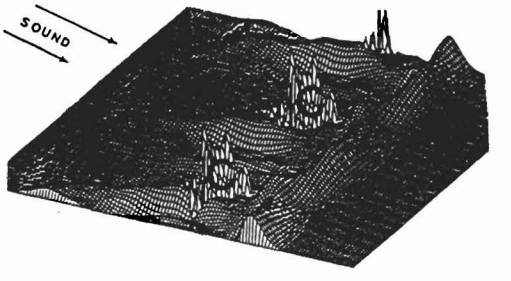

Figure 10: Snapshot of reflection and transmission of Gaussian shaped acoustic pulse by row of air filled double wedge columns in water,pulse was incident from upper left

response of rectangular, cylindrical and double wedge air columns in water to Gaussian and five wavelength sinusoidal wave-packets. To indicate a practical use of this scheme, the acoustic echo of an elastomer layer, filled with air columns and backed by air, was calculated, assuming $\lambda \gg \mu$.

The acoustic responses of the cavities to a Gaussian shaped wave-packet, are shown in scalar, or modulus, form of the dilatation in Figures 8 - 10. The Gaussian pulse is incident from the left in the figures and the time snapshots show the column responses when the pulse has passed the row of air filled cavities, C. The figures show a reflected component moving to the left and the part of the pulse not affected by the cavity to the right. A component which has been slowed at the surface of the cavities through surface relaxation is trailing the main portion of the pulse as expected from surface wave theory [1]. The rapid change in dilatation across the surface indicates that a parabolic

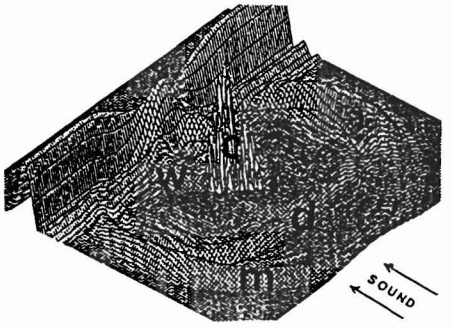

Figure 11: Snapshot of monopole, m , dipole, d, and wavelet, w, responses to Gaussian shaped acoustic pulse, incident from lower right, by air column

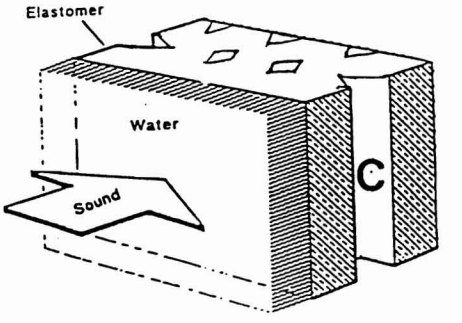

Figure 12: Layer of elastomer containing rows of double and single wedge air columns, basic cell used in computations is shown by dotted lines

approximation to the strain simulates the computed dilatation more accurately than the linear approximation.

The response of a single double wedge shaped air column in water to a Gaussian pulse is shown in Figure 11. The pulse is travelling from lower right to upper left and has passed the double wedge. The primary reflection has moved away from the air column and is followed by the dipole reflection. The corner at the back of the wedge generates a wavelet as is expected from Q_s and theory of surface waves [1]. The cylindrical radial symmetry of the reflections indicate, from consideration of Equation 3 in cylindrical co-ordinates and Equation 6, that sinusoidal waves will be reflected as a damped and a travelling wave.

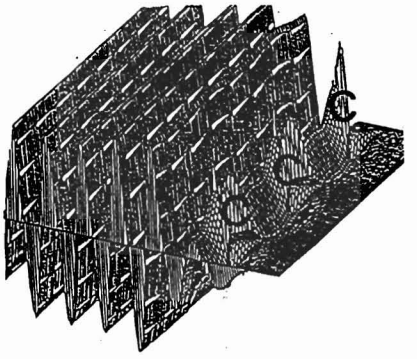

Figure 13: Snapshot of the beginning of the interaction of an acoustic excitation sinusoidal wavepacket with elastomer layer containing double and single wedge air columns

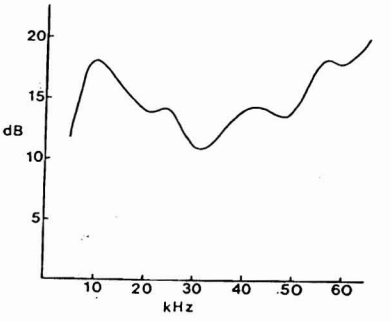

Figure 14: Echo attenuation of elastomer layer containing double and single wedge air columns

Acoustic echo calculations for a selected frequency band of a row of air filled wedges immersed in a fictitious elastomer layer loaded with water, Figure 12, are shown in Figure 13 and Figure 14. The shape, size and spacing of the double and single wedges were chosen to maximize the scatter of short wavelength waves into the coating, resonance absorption of medium wavelength waves in inter-wedge spaces and absorption of longer wavelengths around the cavities.

The reflection coefficient R, shown in Figure 14, was computed from the amplitude of the standing wave Θ_t generated in front of the layer and the amplitude of the incident wave Θ_i through $R = -20\log_{10}\{(\Theta_t - \Theta_i)/\Theta_i\}$.The material properties and layer parameters assumed in the calculations are shown in Table I.

Table 1. MATERIAL PROPERTIES AND GEOMETRY OF ELASTOMER LAYER

Material	Density	Lamé constant	Loss Tangent
	kg/m^3	kg/sm^2	ω β
water	1000	2.25×10^6	0.0
air	1.29×10^{-3}	14.0	0.0
elastomer	1130	2.54×10^6	0.650
Thickness of layer	$0.050m$	Height of double wedge	$0.020m$
Width of wedge	$0.015m$	Separation of wedges	$0.015m$
ω	: angular	excitation frequency	

Analysis indicates that the echo reduction peak at $10kHz$ may be due to monopole resonance, or resonance of circumferential waves around the air column, and the small peak at $22kHz$ may be due to a dipole resonance of the

double wedge air column. The peak at $42kHz$ might be due to a resonance set up between the double wedge and the single wedge of the elastomer layer. The high echo reduction properties of the generic elastomer layer for frequencies greater than $50kHz$ may be attributed to scattering and absorption within the elastomer.

CONCLUSION

The non-linear wave-equation describing the propagation and scatter of a dilatation through piecewise continuous elastic and plastic-visco-elastic media has been presented. The wave-equation has been augmented by the corresponding spectral equation which is able to describe the attenuation and decomposition of travelling waves into damped and propagating components at material boundaries in inhomogeneous media. The numerical analogue is able to model non-linear wave/material interface and discontinuity interactions, and address problems of practical interest in noise engineering.

References

[1] A. Sommerfeld, Mechanics of Deformable Bodies,(Academic Press, New York, 1964).

[2] B. C. H. "The Acoustic Properties of Layered Coatings",MRL Report, MRL-R-1034,(DSTO, March 1988).

[3] R.S. Dunham et al. "Collapse of Various Shaped Cavities in a Pressurized Incompressible Material",ANA-89-0081, ANATECH Research Corp.,March 1989.

[4] J.L. Davis, Wave Propagation in Solid and Fluids,(Springer-Verlag, New York,1987).

[5] H.and B.S.Jeffreys, Mathematical Physics,(Cambridge University Press, Cambridge,1962).

[6] J. A. Doyle, Wave Propagation in Structures,(Springer-Verlag, New York,1988).

[7] D. L. Brown, " A Note on the Numerical Solution of the Wave Equation with Piecewise Smooth Coefficients", Math. Comp.,42, (166), 369-391 (April 1984).

[8] D.A.Sotiropoulus et al. "Quality Assessment of Composite Materials Through Dynamic Characterization",Proceedings COMPO-90,Patras,20-24 August 1990.

[9] R. D. Richtmyer and K. W. Morton, Difference Methods for Initial-Value Problems,(Interscience Publishers,New York,1967).

[10] P. Roache Computational Fluid Dynamics, (Hermosa Publishers, Alberquerque,1982).